

Pair correlation functions and phase separation in a two component point Yukawa fluid

P. Hopkins,* A.J. Archer,† and R. Evans

H.H. Wills Physics Laboratory, University of Bristol, Bristol BS8 1TL, UK

(Dated: March 23, 2021)

We investigate the structure of a binary mixture of particles interacting via purely repulsive (point) Yukawa pair potentials with a common inverse screening length λ . Using the hyper-netted chain closure to the Ornstein-Zernike equations, we find that for a system with ‘ideal’ (Berthelot mixing rule) pair potential parameters for the interaction between unlike species, the asymptotic decay of the total correlation functions crosses over from monotonic to damped oscillatory on increasing the fluid total density at fixed composition. This gives rise to a Kirkwood line in the phase diagram. We also consider a ‘non-ideal’ system, in which the Berthelot mixing rule is multiplied by a factor $(1 + \delta)$. For any $\delta > 0$ the system exhibits fluid-fluid phase separation and remarkably the ultimate decay of the correlation functions is now monotonic for *all* (mixture) state points. Only in the limit of vanishing concentration of either species does one find oscillatory decay extending to $r = \infty$. In the non-ideal case the simple random phase approximation provides a good description of the phase separation and the accompanying Lifshitz line.

PACS numbers:

I. INTRODUCTION

A large class of fluids can be described generically as “big charged particles immersed in a neutralising medium of lighter particles”. Examples include charged colloidal suspensions¹ and dusty plasmas.² A simple model for such systems describes the effective interaction between the bigger particles in terms of a Yukawa (screened Coulomb) pair potential $\phi(r) \propto \exp(-\lambda r)/r$. The effects of the screening due to the neutralising medium are incorporated via the screening parameter λ . Such a Yukawa potential arises in, for example, the linearised Poisson–Boltzmann or Derjaguin–Landau–Verwey–Overbeek theories for the effective potential between spherical charged colloids in solution.¹ The effect of the neutralising medium on the effective potential involves more than the screening effect, as described by the parameter λ . There is an additional effect of charge renormalization, whereby the amplitude of the effective potential $\phi(r)$ is not, as one might perhaps expect from a linear treatment, proportional to Z^2 , where Z is the charge on the big particles (colloids), rather the amplitude of $\phi(r)$ is proportional to \bar{Z}^2 , where $\bar{Z} < Z$ is the renormalised charge.¹

In the present paper we are concerned with a simple model of a *binary* mixture of big charged particles, with both species carrying charges of the same sign, immersed in a neutralising background medium. For a general binary mixture of point Yukawa particles the pair potentials are dependent on six species specific parameters. These are the dimensionless coupling parameters, M_{ij} , and the screening parameters, λ_{ij} , for $i, j = 1, 2$. We assume that both species experience the same screening, $\lambda_{ij} = \lambda$, determined by the background medium (solvent), but that they have different coupling strengths. We can consider the coupling parameters to be proportional to the product of the effective charges of the

species. Thus we define the pair potential as

$$\phi_{ij}(r) = \frac{M_{ij}\epsilon \exp(-\lambda r)}{\lambda r}, \quad (1)$$

where ϵ denotes the overall energy scale, and all three potentials are repulsive: $M_{ij} > 0$. As usual it is assumed that the inter-species parameters are related to those for like particles.³ The Berthelot mixing rule sets $M_{12} = \sqrt{M_{11}M_{22}}$. This choice could correspond to ions with charge \bar{Z}_i , with $\bar{Z}_1, \bar{Z}_2 > 0$, immersed in a medium with an inverse screening length λ . In order to generalise this mixing rule we introduce a non-ideality parameter $\delta > 0$ such that $M_{12} = (1 + \delta)\sqrt{M_{11}M_{22}}$. The case $\delta = 0$ clearly corresponds to the ideal system. The non-ideal case $\delta \neq 0$ can be viewed as arising from charge screening effects in the double layer of condensed counter ions on the surface of the particles. The double layer leads to an effective renormalisation of the particle charge and strongly affects the particle interactions.¹ One should expect that for some positive δ that the energy penalty incurred for unlike species to be neighbours should lead to fluid-fluid demixing at high densities; such behaviour is found in models of soft-core fluids where positive non-additivity gives rise to demixing.^{4,5,6,7}

Binary mixtures of H^+ and He^{++} in a neutralising medium are expected to phase separate at temperatures and pressures of astrophysical interest – see Ref. 8. In this system the phase separation is thought to be due to charge neutralisation being less efficient in the mixture than in the pure phases. We believe that some of the complex screening effects associated with such systems may be incorporated in a simple model such as ours, via the parameter δ . Non-ideal charge renormalisation effects may also be present in binary suspensions of colloids. Charge renormalisation may be affected by the local concentrations of the different species of colloids and counterions in very subtle ways leading to the possibility

that the amplitude of $\phi_{12}(r)$ may not be proportional to $\bar{Z}_1\bar{Z}_2$. Such effects would be mimicked using our simple model. It may be the case that in some colloidal fluid mixtures $\delta > 0$, or it may be that in other cases $\delta < 0$, i.e. non-ideal charge renormalization effects may favour mixing. However, in the present paper we investigate only the cases $\delta = 0$ and $\delta > 0$. Using the accurate hyper-netted chain (HNC) approximation we find that for the case $\delta = 0$ the total pair correlation functions $h_{ij}(r)$ exhibit crossover from monotonic to exponentially damped oscillatory asymptotic decay, $r \rightarrow \infty$, on increasing the total density of the fluid mixture at fixed composition. This scenario is equivalent to that observed in the one-component point Yukawa fluid (OCY).⁹ However, in the non-ideal case, an *infinitesimal* positive δ can give rise to fluid-fluid phase separation at a sufficiently large total density. Moreover we find that the fluid structure is changed profoundly from that pertaining to $\delta = 0$, i.e. for all thermodynamic state points, apart from the limits of pure species 1 and 2, the ultimate, $r \rightarrow \infty$, decay of correlations is monotonic. We find that for the particular choice $\delta = 0.1$ the very simple random phase approximation (RPA) provides a good account of the fluid-fluid binodal and spinodal obtained from the HNC but a poor account of the detailed behaviour of the correlation functions.

The paper is arranged as follows: In Secs. II and III we remind readers of the HNC and RPA integral equations and some basic results from the theory of the asymptotic decay of pair correlation functions in binary mixtures. Sec. IV describes results for $h_{ij}(r)$ and for the poles of the Fourier transforms $\hat{h}_{ij}(q)$ obtained from numerical solutions of the HNC closure approximation. Within the RPA we are able to calculate the corresponding poles analytically and we compare these results with those from the HNC. The pole analysis enables us to determine the behaviour of $h_{ij}(r)$ at intermediate range, as well as at longest range, $r \rightarrow \infty$. Particular attention is paid to the behaviour of the correlation functions in the limit where the density of species 2, $\rho_2 \rightarrow 0$. In Sec. V we present phase diagrams, in the composition, total density plane, along with Lifshitz lines for the partial structure factors, obtained from both the HNC and RPA. We draw some conclusions in Sec. VI.

II. CLOSURE OF THE OZ EQUATIONS

Our starting point for determining the fluid structure is the mixture Ornstein-Zernike (OZ) equation³ which relates the total correlation functions, $h_{ij}(r) = g_{ij}(r) - 1$, where $g_{ij}(r)$ are the radial distribution functions, to a set of pair direct correlation functions, $c_{ij}(r)$:

$$h_{ij}(r_{12}) = c_{ij}(r_{12}) + \sum_{k=1}^2 \rho_k \int d^3r_3 c_{ik}(r_{13}) h_{kj}(r_{32}), \quad (2)$$

where $r_{ij} = |\mathbf{r}_i - \mathbf{r}_j|$ and ρ_k is the bulk density of species k . These equations can be viewed as defining the pair direct correlation functions. In order to determine the fluid structure a second relation, or closure, is required.

The simplest closure germane to the present model is the random phase approximation (RPA): $c_{ij}^{RPA} = -\beta\phi_{ij}(r)$ with $\beta = (k_B T)^{-1}$, which is strictly valid only for $r \rightarrow \infty$. Although this approximation is inadequate for hard-core model systems, it has been shown that the RPA becomes accurate for some soft-core systems at intermediate densities and exact at high densities.^{4,5,6,7,10,11,12} An important advantage of the RPA is that it does provide an analytical solution for correlation functions and for thermodynamic properties which may provide valuable physical insight into fluid behaviour.

A more accurate approximation is the hyper-netted chain (HNC) approximation. The exact closure of the OZ equations can be expressed as:

$$g_{ij}(r) = \exp(-\beta\phi_{ij}(r) + h_{ij}(r) - c_{ij}(r) - b_{ij}(r)), \quad (3)$$

where $-b_{ij}(r)$ is an unknown bridge function.³ The HNC simply sets this bridge function to zero for all r . It is found to be accurate for long-ranged or soft-core potentials,^{3,8,10} although it may fail in the neighbourhood of a spinodal. For the one-component (point) Yukawa fluid it is known that the HNC is remarkably accurate for small coupling parameters.^{9,13} In order to determine the correlation functions within the HNC we use a standard iterative procedure. In what follows, we fix the reduced temperature $T^* = (\beta\epsilon)^{-1}$ so that the state of the system is determined by the total density, $\rho = \rho_1 + \rho_2$, and the species concentrations $x_i = \rho_i/\rho$.

III. ASYMPTOTIC DECAY OF CORRELATION FUNCTIONS

There are two procedures for determining the asymptotic, $r \rightarrow \infty$, behaviour of the total correlation functions. One is to examine directly the numerical solutions for $h_{ij}(r)$. The alternative method is to input the direct correlation functions (in the present case from either the RPA or HNC closures) into the set of OZ equations (2) and perform an asymptotic analysis. The OZ equations can be solved formally in Fourier space and the solution written as

$$\hat{h}_{ij}(q) = \frac{N_{ij}(q)}{D(q)}, \quad (4)$$

where $\hat{h}_{ij}(q)$ denotes the three-dimensional Fourier transform of $h_{ij}(r)$. The three functions share the same denominator

$$D(q) = [1 - \rho_1 \hat{c}_{11}(q)][1 - \rho_2 \hat{c}_{22}(q)] - \rho_1 \rho_2 \hat{c}_{12}(q)^2, \quad (5)$$

but the numerators are dependent on the indices:

$$\begin{aligned} N_{11}(q) &= \hat{c}_{11}(q) + \rho_2[\hat{c}_{12}(q)^2 - \hat{c}_{11}(q)\hat{c}_{22}(q)], \\ N_{22}(q) &= \hat{c}_{22}(q) + \rho_1[\hat{c}_{12}(q)^2 - \hat{c}_{11}(q)\hat{c}_{22}(q)], \\ N_{12}(q) &= N_{21}(q) = \hat{c}_{12}(q). \end{aligned} \quad (6)$$

From the inverse Fourier transform it follows that:

$$rh_{ij}(r) = \frac{1}{2\pi^2} \int_0^\infty dq q \sin(qr) \hat{h}_{ij}(q). \quad (7)$$

Using Eq.(4) and assuming that the singularities of $\hat{h}_{ij}(q)$ for the present Yukawa systems are simple poles we are able to proceed via the residue theorem.¹⁴ Performing contour integration around a semicircle in the upper half of the complex q plane, we write the total correlation functions as a sum of contributions from the poles enclosed:

$$rh_{ij}(r) = \sum_n A_n^{ij} \exp(iq_n r), \quad (8)$$

where q_n satisfies $D(q_n) = 0$ and A_n^{ij} is the amplitude associated with the pole q_n . This amplitude is related to the residue R_n^{ij} of $qN_{ij}(q)/D(q)$ by $A_n^{ij} = R_n^{ij}/2\pi$. The poles are either purely imaginary, $q = i\alpha_0$, or occur as a conjugate complex pair $q = \pm\alpha_1 + i\tilde{\alpha}_0$.¹⁴

In general there are an infinite number of poles and contributions from many of these are required to account for the behaviour of $h_{ij}(r)$ at small r . However, the ultimate, $r \rightarrow \infty$, decay of $h_{ij}(r)$ is determined by the pole that gives the slowest exponential decay, i.e. the pole with the smallest imaginary part. This is referred to as the leading order pole. If the leading order pole is purely imaginary then $rh_{ij}(r)$ decays exponentially, $rh_{ij}(r) \sim A_{ij} \exp(-\alpha_0 r)$, as $r \rightarrow \infty$. On the other hand, if the leading order poles are a conjugate complex pair, then the sum of contributions from this pair of complex poles gives damped oscillatory decay, $rh_{ij}(r) \sim 2A_{ij} \exp(-\tilde{\alpha}_0 r) \cos(\alpha_1 r - \tilde{\theta}_{ij})$, where A_{ij} and $\tilde{\theta}_{ij}$ denote the amplitude and phase respectively.¹⁴

Note that whereas the wavelength $2\pi/\alpha_1$ and the decay lengths α_0^{-1} or $\tilde{\alpha}_0^{-1}$ are the same for all $h_{ij}(r)$, the amplitudes and phases do depend on the indices ij .¹⁴ However, general considerations demand $A_{12}^2 = A_{11}A_{22}$ or $\tilde{A}_{12}^2 = \tilde{A}_{11}\tilde{A}_{22}$ and $2\tilde{\theta}_{12} = \tilde{\theta}_{11} + \tilde{\theta}_{22}$.¹⁴ In the next section we shall employ the RPA and the HNC closures to investigate the ultimate, $r \rightarrow \infty$, decay of $h_{ij}(r)$ and the behaviour of $h_{ij}(r)$ at intermediate distances r . Note that the values of the amplitudes are relevant in determining which pole or conjugate complex pair provides the dominant contribution to $h_{ij}(r)$ in the intermediate regime.

IV. RESULTS FOR PAIR CORRELATION FUNCTIONS

In Fig. 1 we display the radial distribution functions $g_{ij}(r)$, obtained from the HNC closure, for the state point

$\rho\lambda^{-3} = 0.5$, $x_2 = 0.5$ and $T^* = 1$. The coupling parameters are fixed at $M_{11} = 1$, and $M_{22} = 4$. Fig. 1(a) corresponds to ideal (Berthelot) mixing, $\delta = 0$, Fig. 1(b) has $\delta = 10^{-5}$, weak non-ideality, while Fig. 1(c) has $\delta = 0.1$. In all cases the $g_{ij}(r)$ appear structureless but the expanded scales of the insets reveal the nature of the intermediate and long range decay of the pair correlation functions. For $\delta = 0$, $rh_{ij}(r)$ shows exponentially damped oscillatory decay extending to arbitrarily large separations r . By contrast, for $\delta = 10^{-5}$, there are several oscillations at small r and $rh_{ij}(r)$ decays monotonically (exponentially) for $\lambda r \gtrsim 8$. For $\delta = 0.1$ the monotonic decay extends from $\lambda r \simeq 3$. Clearly the choice of δ has a profound influence on the behaviour of the pair correlation functions. If one fixes the concentration at $x_2 = 0.5$ and reduces the total density ρ one finds that for $\delta = 0$ there is a crossover from the exponentially damped oscillatory behaviour of $rh_{ij}(r)$ shown in Fig. 1(a) to monotonic (exponential) decay similar shown to that in Fig. 1(c), near $\rho\lambda^{-3} \simeq 0.05$. Such crossover is found in the OCY on reducing the density at fixed T^* .⁹ The scenario is different for $\delta > 0$. On reducing the density at fixed $x_2 = 0.5$ the $h_{ij}(r)$ are similar to those for $\rho\lambda^{-3} = 0.5$; the decay remains monotonic. Similar features are found for other values of the concentration provided $x_1, x_2 \neq 0$. If $x_2 = 0$ or 1 then one recovers the OCY which exhibits crossover as mentioned above.

In order to understand these results emanating from the full numerical solution of the HNC closure we turn to the asymptotic (pole) analysis of Sec. III. It is convenient to begin with the simple RPA treatment before discussing the more sophisticated HNC results.

A. Poles in the RPA

The advantage of the RPA is that the pair direct correlation functions and their Fourier transforms, $\hat{c}_{ij}(q)$, are given analytically. This means that the poles can be determined analytically. Using the definition of the RPA it follows from Eq. (1) that

$$\hat{c}_{ij}^{RPA}(q) = -\frac{4\pi M_{ij}}{\lambda T^*} \frac{1}{(\lambda^2 + q^2)}. \quad (9)$$

Substituting this form into Eq. (5) we can solve for the zeros of $D(q)$, i.e. the poles, q_n , at each state point. We find that within the RPA there are only two poles. Both are purely imaginary and are given by

$$\alpha_0 = \sqrt{\frac{2\pi\rho}{\lambda T^*} \left(M_0 \pm \sqrt{M_0^2 + M_\delta} \right) + \lambda^2}. \quad (10)$$

where we have introduced $M_0 = x_1 M_{11} + x_2 M_{22}$ and $M_\delta = 4x_1 x_2 M_{11} M_{22} (2 + \delta)\delta$.

For $\delta = 0$ this gives an imaginary pole with $\alpha_0^+ \geq \lambda$, pertaining to the positive sign, and a ‘false’ solution obtained with the negative sign giving $\alpha_0 = \lambda$ for all

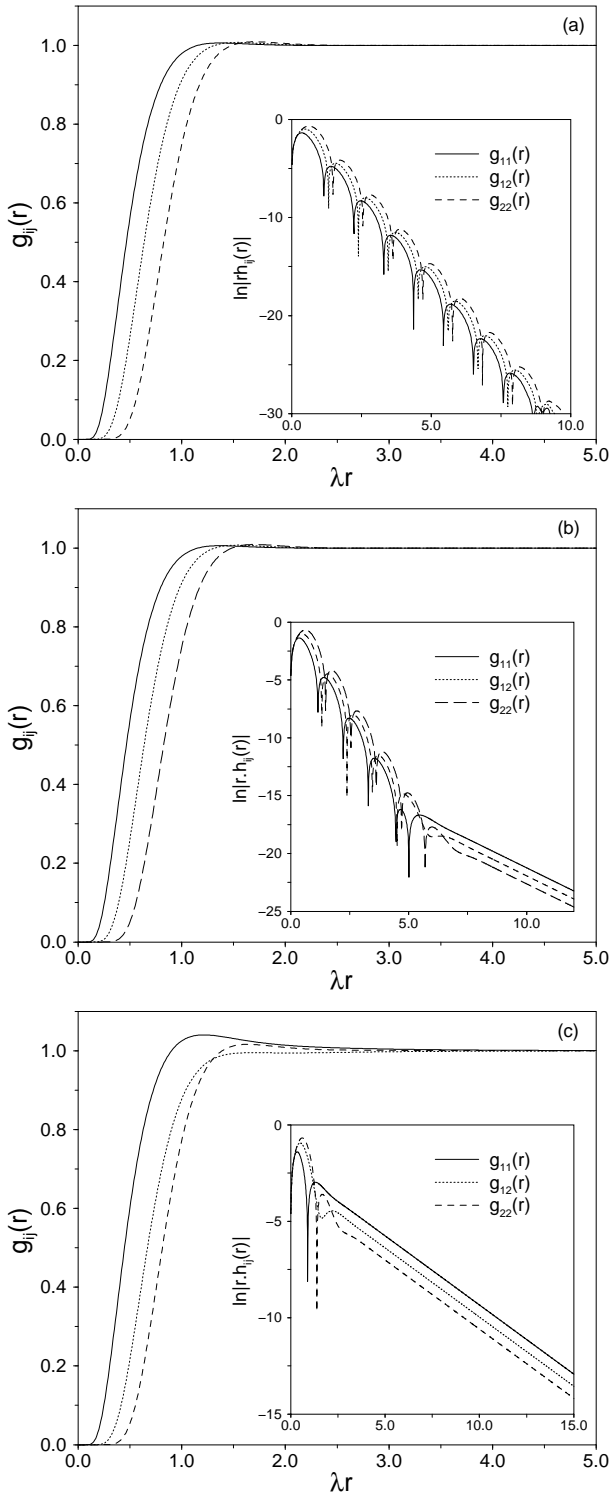


FIG. 1: Pair correlation functions for the state point $\rho\lambda^{-3} = 0.5$, $x_2 = 0.5$ and $T^* = 1$, calculated from the HNC closure, using the coupling parameter ratio $M_{22}/M_{11} = 4$. Main figures show radial distribution functions, $g_{ij}(r)$, and insets show $\ln|r h_{ij}(r)|$ versus λr . a) $\delta = 0$. Exponentially damped oscillations extend to infinity. b) $\delta = 10^{-5}$. For $\lambda r \gtrsim 8$, $r h_{ij}(r)$ exhibit monotonic (exponential) decay. c) $\delta = 0.1$. Monotonic decay now develops for $\lambda r \gtrsim 3$.

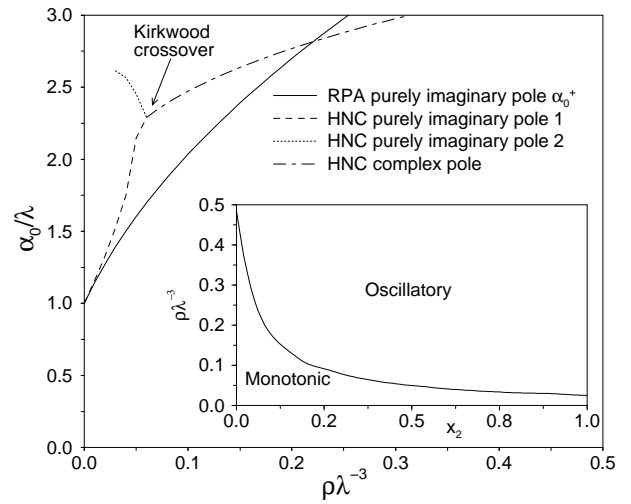


FIG. 2: The imaginary components of leading order poles, α_0 , calculated along a path in the phase diagram of increasing density, ρ , for fixed $x_2 = 0.5$ and $T^* = 1$. $\delta = 0$, corresponding to an ‘ideal’ mixture. The RPA solution, Eq. (10), consists of a single, purely imaginary pole, α_0^+ , which increases steadily with density from $\alpha_0/\lambda = 1$. Within the HNC closure, at low densities ρ , the two leading order poles are both purely imaginary. As the density is increased the first imaginary pole ascends and the second imaginary pole descends and, at the Kirkwood crossover point, coalesce becoming a conjugate complex pair $q = \pm\alpha_1 + i\alpha_0$. Increasing the density further both the real and imaginary parts of the complex poles increase. Thus the Kirkwood point marks the boundary between monotonic (at small $\rho\lambda^{-3}$) and damped oscillatory asymptotic decay. The inset shows the Kirkwood line, separating the two types of decay, plotted in the concentration-total density phase diagram.

state points. The imaginary pole is analogous to that found in the RPA solution for the OCY. Fig. 2 shows how this pole ascends from $\alpha_0 = \lambda$ at $\rho = 0$ as the density ρ is increased, along a line of constant concentration, $x_2 = 0.5$, at fixed temperature $T^* = 1$.

By calculating the residues one can show (see Eq. (14) below) that the ‘false’ pole $\alpha_0 = \lambda$ makes no contribution to $h_{ij}(r)$, i.e. for $\delta = 0$ the corresponding amplitude $A_{ij}^- = 0$ and

$$r h_{ij}^{RPA}(r) = A_{ij}^+ \exp(-\alpha_0^+ r) \quad (11)$$

where α_0^+ is given by Eq. (10), with the positive sign, and the amplitudes are independent of the density¹⁵

$$A_{ij}^+ = -\frac{M_{ij}}{\lambda T^*}. \quad (12)$$

The situation is quite different for $\delta > 0$. We find that the pole with $\alpha_0^+ > \lambda$ is modified slightly by the addition of a (relatively) small positive term. More significantly we find that the solution with the negative sign now corresponds to a second pole which descends from $\alpha_0^- = \lambda$ eventually reaching zero as the density is increased – see

Fig. 3. The locus of points in the phase diagram for which $\alpha_0^- = 0$ is the spinodal, where the $\hat{h}_{ij}(q)$ (or the partial structure factors) diverge in the limit $q \rightarrow 0$, indicating that the system is undergoing fluid-fluid demixing. Note that this second ‘spinodal’ pole exists only for the mixture states, i.e. for $x_1, x_2 \neq 0$; in the pure states it reverts to the ‘false’ solution $\alpha_0 = \lambda$. The behaviour of this pole is shown for fixed $x_2 = 0.5$, and increasing density in Fig. 3.

The ‘spinodal’ pole is present for arbitrarily small positive δ . Therefore the RPA predicts that the system will undergo phase separation provided there is any degree of positive non-ideality in the pair potentials. This behaviour is reflected in the asymptotic decay of the total correlation functions. For $\delta > 0$,

$$r h_{ij}^{RPA}(r) = A_{ij}^+ \exp(-\alpha_0^+ r) + A_{ij}^- \exp(-\alpha_0^- r) \quad (13)$$

with $\alpha_0^- < \lambda < \alpha_0^+$, which follows from Eq. (10). The particularly simple forms of Eqs. (11) and (13) are a consequence of the RPA.¹⁵ The amplitudes are

$$A_{ij}^\pm = -\frac{1}{4\lambda T^*} \frac{2M_{ij} \left(M_0 \pm \sqrt{M_0^2 + M_\delta} \right) + \delta_{ij} M_\delta / x_i}{M_0 + M_\delta / \left(M_0 \pm \sqrt{M_0^2 + M_\delta} \right)}, \quad (14)$$

where superscript \pm refers to the sign in front of the square root and we use the compound parameters M_0 and M_δ defined previously. δ_{ij} is the Kronecker delta. As the ultimate decay is determined by the pole with the smallest imaginary part, the ‘spinodal’ pole α_0^- must determine the ultimate decay of $h_{ij}(r)$ for any $\delta > 0$. For very small $\delta > 0$, α_0^- lies very close to λ until the reduced density $\rho\lambda^{-3}$ reaches very large values, i.e. the spinodal is shifted to very large densities as $\delta \rightarrow 0$. In these circumstances the relative magnitude of the amplitudes A_{ij}^+ and A_{ij}^- becomes important; note that α_0^+ depends only weakly on δ . For a given state point the amplitude of the ‘spinodal’ pole A_{ij}^- decreases relative to A_{ij}^+ as $\delta \rightarrow 0$ and one must go to increasing values of r before the ‘spinodal’ pole provides the dominant contribution to $h_{ij}(r)$. At intermediate r the contribution from α_0^+ determines the decay behaviour.

B. Poles in the HNC

For the OCY the HNC predicts a crossover line in the (ρ, T) plane separating a region where the asymptotic decay of $h(r)$ is damped oscillatory from that where it is monotonic. The crossover takes place via the coalescence of two imaginary poles to form a complex pole as the density is increased at fixed temperature T .⁹ The mechanism is equivalent to that discussed first by Kirkwood in pioneering studies of strong electrolytes.¹⁶ Thus for the pure species we take the results of Ref. 9 and read off the crossover values of $\rho\lambda^{-3}$. For $T^* = 1$ and $x_2 = 0$ (pure species 1) crossover occurs at $\rho\lambda^{-3} \approx 0.47$ whereas for

$x_2 = 1$ (pure species 2) this occurs at $\rho\lambda^{-3} \approx 0.025$. If we vary the concentration between these limiting values (at fixed $T^* = 1$) we expect to find a crossover line in the $(x_2, \rho\lambda^{-3})$ plane. We determined this line by calculating the poles of $\hat{h}_{ij}(q)$, i.e. the zeros of $D(q)$, using the same numerical procedure as in Ref. 9 for the OCY.

The pair direct correlation functions $c_{ij}(r)$ are obtained from the full solutions of the HNC integral equations. In order to ensure convergence of the integrals which determine the poles we follow the procedure given in Refs. 9 and 17. For $r \rightarrow \infty$, $c_{ij}(r) \rightarrow -M_{ij} \exp(-\lambda r) / (\lambda T^* r)$, so we define a short range direct correlation function $c_{ij}^{sr}(r)$:

$$c_{ij}^{sr}(r) \equiv c_{ij}(r) + \frac{M_{ij} \exp(-\lambda r)}{\lambda T^* r}. \quad (15)$$

Fourier transforming we find

$$\hat{c}_{ij}(q) = \hat{c}_{ij}^{sr}(q) - \frac{4\pi M_{ij}}{\lambda T^*} \frac{1}{(q^2 + \lambda^2)}, \quad (16)$$

which can be substituted into Eq. (5). $D(q)$ is separated into its real and imaginary components, and the equation $D(q) = 0$ is solved numerically using a Newton-Raphson procedure. In general, the relevant integrals converge only for complex q such that $\Im[q] \lesssim 2\alpha_0$, where α_0 is the imaginary part of the leading order pole.¹⁷ It follows that only a few poles can be calculated; the remaining poles are situated outside this region of convergence. Fortunately the poles relevant for determining the basic features of the decay of correlations can be obtained.

For the case $\delta = 0$ we find that for all x_2 the leading poles exhibit Kirkwood cross-over mimicking that in the OCY.⁹ At very low densities we find an imaginary pole (dashed line in Fig. 2) that ascends from $\alpha_0 = \lambda$ as we increase the density ρ at constant concentration, and is initially similar to the RPA. At slightly higher densities a second imaginary pole (dotted line) moves into the region of convergence and descends as ρ increases. These two poles move towards each other and then, at the Kirkwood point, coalesce. On increasing the density further, one finds a conjugate complex pair whose real and imaginary parts both increase with ρ (dash-dotted line). Fig. 2 shows the imaginary parts of the relevant poles as they undergo the Kirkwood cross-over. The locus of points for which the poles coalesce, the Kirkwood line, is shown in the inset to Fig. 2. Below this line the asymptotic decay of $r h_{ij}(r)$ is pure exponential and above the line it is exponentially damped oscillatory. One sees that the state point $x_2 = 0.5$ and $\rho\lambda^{-3} = 0.5$, which corresponds to the results for $h_{ij}(r)$ in Fig. 1(a), lies deep within the oscillatory region so one expects to find oscillations extending to $r \rightarrow \infty$.

Fig. 3 displays the corresponding plots of α_0 for $\delta = 0.1$. Now there are *three* purely imaginary poles at low densities. Two of these mimic closely what is found for $\delta = 0$, i.e. they coalesce and form a complex pole at a Kirkwood point that is not far removed from the corresponding point for $\delta = 0$. Once again one of these poles

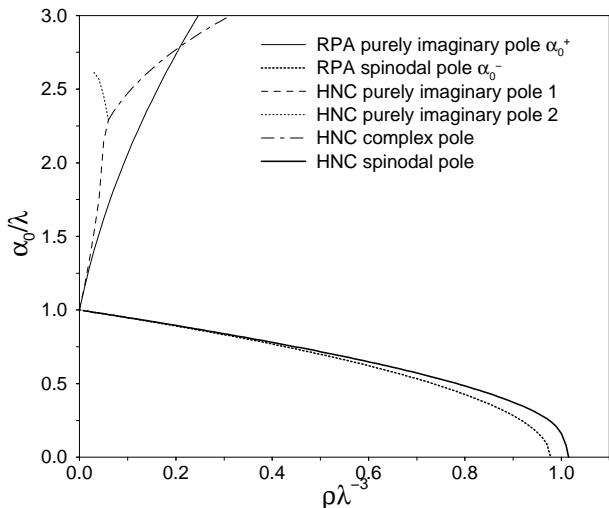


FIG. 3: As in Fig. 2 but now for $\delta = 0.1$. Within the RPA the imaginary pole α_0^+ , is shifted by only a small amount from the case $\delta = 0$. A second purely imaginary pole α_0^- is introduced which decreases from λ to zero as ρ is increased; $\alpha_0^- = 0$ corresponds to the spinodal. Since $\alpha_0^- < \alpha_0^+$ this ‘spinodal’ pole determines the ultimate decay of the total correlation functions. Within the HNC closure the Kirkwood mechanism is still present and the crossover point is largely unchanged from the case $\delta = 0$. However, a ‘spinodal’ pole is introduced which follows closely the corresponding RPA pole α_0^- . It follows that for *all* densities the ultimate decay of the total correlation functions is monotonic. Although the Kirkwood crossover is present it does not involve the leading order ‘spinodal’ pole and therefore does not influence the ultimate decay.

(dashed line) lies close to the RPA solution α_0^+ for very small values of $\rho\lambda^{-3}$. The third pole follows closely the RPA ‘spinodal’ pole α_0^- ; it decreases slowly with increasing $\rho\lambda^{-3}$ for small densities before decreasing rapidly to zero at the spinodal point which is at $\rho\lambda^{-3} \approx 1.01$, slightly higher than the value $\rho\lambda^{-3} = 0.98$ found from the RPA. We refer to the third pole as the HNC ‘spinodal’ pole.

It is evident from Fig. 3 that within the HNC, as in the RPA, the purely imaginary ‘spinodal’ pole with $\alpha_0 < \lambda$ will determine the ultimate decay of $h_{ij}(r)$ which will be monotonic for all densities provided $0 < x_2 < 1$. The ultimate decay cannot be oscillatory. Although there is still a Kirkwood-like crossover, this now involves higher order poles rather than the leading order poles, which was the case for $\delta = 0$. The corresponding crossover line is shown as the dotted line in the $(x_2, \rho\lambda^{-3})$ phase diagram for $\delta = 0.1$ displayed in Fig. 4. Note that the line lies far below the HNC spinodal (diamonds). Crossover does not influence the ultimate decay of $h_{ij}(r)$ which is stubbornly monotonic.

Of course, this does not mean that we do not find oscillations at intermediate r . For densities larger than the crossover value the HNC pole analysis predicts, for

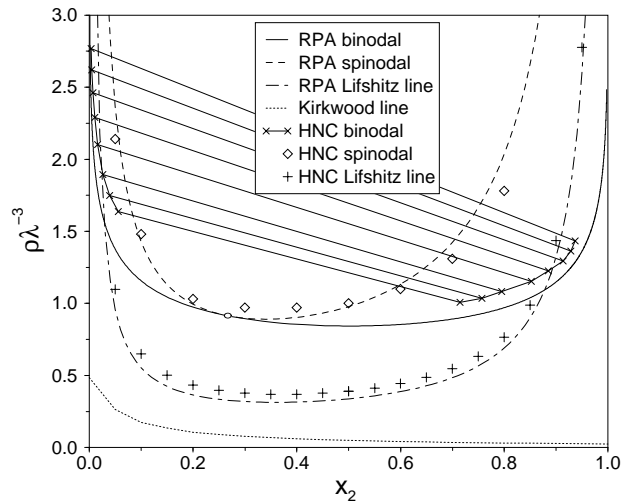


FIG. 4: Phase diagram for the binary Yukawa system with $M_{22}/M_{11} = 4$, $T^* = 1$ and $\delta = 0.1$. The system exhibits phase separation within both the RPA and HNC closures. The RPA spinodal (dashed curve) meets the RPA binodal (solid curve) at the critical point \circ . The HNC spinodal points (diamonds) were calculated by extrapolating the ‘spinodal’ pole to zero along lines of constant concentration and increasing density. The HNC binodal was calculated using the method outlined in the text; the straight segments are tie-lines connecting co-existing fluid phases denoted by crosses and correspond to the following reduced pressures $\beta P\lambda^{-3} = 20, 22, 25, 30, 35, 40, 45$ and 50 . Also shown is the Lifshitz line for $S_{NN}(q)$ calculated in both the RPA (dash-dotted) and HNC (crosses). The dotted line at low density denotes Kirkwood crossover from monotonic to oscillatory decay of correlation functions. However for $\delta > 0$ and $0 < x_2 < 1$ the true asymptotic decay remains monotonic even for states above the line – see text.

$r \rightarrow \infty$,

$$rh_{ij}(r) \sim A_{ij} \exp(-\alpha_0 r) + 2\tilde{A}_{ij} \exp(-\tilde{\alpha}_0 r) \cos(\alpha_1 r - \tilde{\theta}_{ij}) \quad (17)$$

with $\alpha_0 < \tilde{\alpha}_0$. Provided $\tilde{A}_{ij} \gg A_{ij}$ and we are not close to the spinodal ($\alpha_0 = 0$) the oscillatory contribution will be significant in the intermediate regime.

An example is given in Fig. 5 which compares the full numerical result for $h_{22}(r)$ with the contribution given by Eq. (17) for a statepoint ($x_2 = 0.99, \rho\lambda^{-3} = 0.05$) where the amplitude of the ‘spinodal’ pole is very small. On a normal scale plot $h_{22}(r)$ is well-described by the contribution from a single conjugate complex pair of poles, i.e. by the second term in Eq. (17). This contribution is oscillatory, albeit with a small amplitude. The inset to Fig. 5 plots $\ln|r h_{22}(r)|$ for a larger range of λr . Now the oscillations are manifest but we observe monotonic (exponential) decay, described accurately by the first term in Eq. (17), for $\lambda r \gtrsim 14$ (dotted line). As the amplitude λA_{22} of the ‘spinodal’ pole contribution is $\sim 10^{-6}$ this contribution does not become significant until large separations r . Of course such a contribution might be impossible to detect experimentally or in simulations. We conclude that although a pair correlation function might

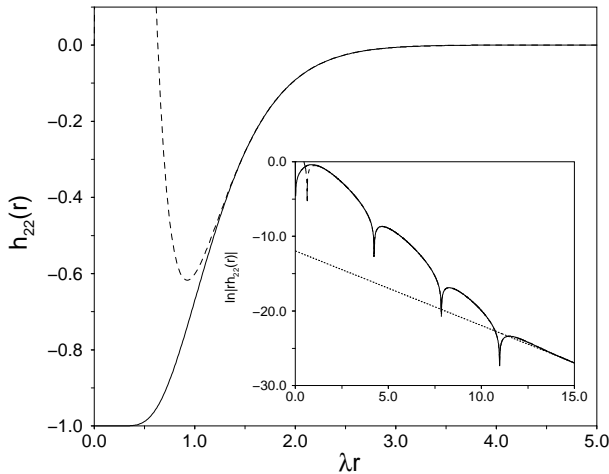


FIG. 5: Comparison between results of the full HNC solution for $h_{22}(r)$ (solid line) and the contributions of the lowest order poles for state point $\rho\lambda^{-3} = 0.05$, $x_2 = 0.99$ and parameters $M_{22}/M_{11} = 4$, $T^* = 1$ and $\delta = 0.1$. Note this point lies above the Kirkwood crossover line in Fig. 4. The main figure shows that the decay of $h_{22}(r)$ is well described by the contribution from a single pair of conjugate complex poles (dashed line) ($\tilde{\alpha}_0/\lambda_0 = 2.269$, $\alpha_1/\lambda = 0.8723$). On this scale the contribution from the purely imaginary pole is vanishingly small. In the inset the plot of $\ln|h_{22}(r)|$ versus λr (solid line) shows that although the oscillatory contribution (dashed line – visible only in top left hand corner) describes $h_{22}(r)$ accurately for intermediate range, the contribution from the ‘spinodal’ pole (dotted line) ($\alpha_0/\lambda = 0.9993$) determines the decay for $\lambda r \gtrsim 14$. Thus the sum of contributions from the oscillatory and ‘spinodal’ poles (dot-dashed) given by Eq. (17) is very accurate in the range $1.5 < \lambda r < \infty$.

exhibit many oscillations, the ultimate decay can still be monotonic. Note that for a state point closer to the spinodal, such as in Fig. 1(c) where $x_2 = 0.5$, $\rho\lambda^{-3} = 0.5$ and $\alpha_0/\lambda \approx 0.72$, the purely exponential contribution in Eq. (17) dominates for $\lambda r \gtrsim 3$.

For a pure (one component) fluid there is no ‘spinodal’ pole; within the HNC the Kirkwood crossover occurs between leading-order poles. Therefore, on the axes $x_2 = 0$ and $x_1 = 0$ in Fig. 4 $h_{ii}(r)$ must decay in an oscillatory fashion as $r \rightarrow \infty$, provided we consider states above the Kirkwood crossover densities. However, as we increase x_2 (or x_1) infinitesimally the ‘spinodal’ pole makes a non-vanishing contribution to the correlation functions and forces the ultimate decay of $h_{ij}(r)$ to be monotonic. In order to understand the evolution of this behaviour we must consider the amplitudes, A_{ij} , of the ‘spinodal’ pole as the concentration x_2 vanishes along a line of constant total density. Fig. 6 shows results for $\rho\lambda^{-3} = 0.5$, a density that lies just above the Kirkwood crossover value, $\rho\lambda^{-3} \sim 0.47$, for the pure fluid. The ‘spinodal’ pole $\alpha_0/\lambda \rightarrow 1^-$ as $x_2 \rightarrow 0$, and the accompanying amplitudes A_{11} (positive) and A_{12} (negative) both vanish, as power laws, in this limit. It follows that the ‘spinodal’ pole makes contributions to $h_{11}(r)$ and $h_{12}(r)$ that become

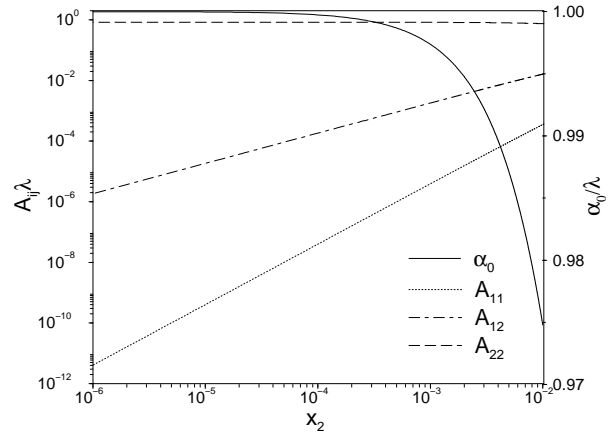


FIG. 6: The HNC ‘spinodal’ pole α_0 and corresponding amplitudes A_{ij} as a function of concentration x_2 along a path of constant density $\rho\lambda^{-3} = 0.5$, for $T^* = 1$, and $\delta = 0.1$. As $x_2 \rightarrow 0$, $\alpha_0/\lambda \rightarrow 1^-$, $A_{11}, A_{12} \rightarrow 0$ but $A_{22}\lambda$ tends to 0.84. Note that A_{12} is negative and its magnitude is plotted here. The amplitudes obey the rule $A_{12}^2 = A_{11}A_{22}$ – see text.

vanishingly small in a continuous fashion, as $x_2 \rightarrow 0$. Thus for very small concentrations $h_{11}(r)$ and $h_{12}(r)$ appear oscillatory until extremely large values of λr where the ‘spinodal’ pole will dictate the final (monotonic) decay of these functions.

The amplitude A_{22} of the minority component, species 2, has a different variation. As shown in Fig. 6, λA_{22} remains almost constant as the concentration is reduced and tends to a non-zero value (0.84) at $x_2 = 0$. At first sight this result is a little surprising. However we should recall that physical observables such as probability distributions or the liquid structure factors involve the product $\rho_2 h_{22}(r)$ which vanishes as $x_2 \rightarrow 0$. We confirmed that our numerical results for the amplitudes satisfy the rule¹⁴ $A_{12}^2 = A_{11}A_{22}$ mentioned in Sec. III.

At this point it is instructive to return to the RPA ‘spinodal’ pole. Recall that α_0^- is given by Eq. (10) and the corresponding amplitudes by Eq. (14). If we Taylor expand around $x_2 = 0$ we find that

$$\alpha_0^- = \lambda \left(1 - \frac{2\pi\rho M_{22}\delta(2+\delta)}{\lambda^3 T^*} x_2 \right) + O(x_2^2), \quad (18)$$

A_{11}^- and A_{12}^- decay to zero as power laws in x_2 , and that A_{22}^- tends to a constant, i.e.

$$\begin{aligned} A_{11}^- &= \frac{M_{22}^2(1+\delta)^2(2+\delta)\delta}{\lambda T^* M_{11}} x_2^2 + O(x_2^3), \\ A_{12}^- &= -\frac{M_{22}^{3/2}(1+\delta)(2+\delta)\delta}{\lambda T^* M_{11}^{1/2}} x_2 + O(x_2^2), \\ A_{22}^- &= \frac{M_{22}(2+\delta)\delta}{\lambda T^*} + O(x_2). \end{aligned} \quad (19)$$

In the limit $x_2 \rightarrow 0$, $\lambda A_{22}^- = M_{22}(2+\delta)\delta/T^*$ which takes the value 0.84 for the present choice of parameters:

$M_{22} = 4$, $\delta = 0.1$ and $T^* = 1$. This is the same limiting value of the amplitudes as obtained in the HNC. Indeed we find that the RPA results for α_0^- and for the amplitude A_{ij}^- are almost identical to those from the numerical HNC results for concentrations $x_2 \lesssim 10^{-4}$. Thus, numerically, the limiting behaviour predicted by Eqs. (18) and (19) pertains to the HNC as well as to the RPA. Note that the coefficients of the leading order terms in Eq. (19) are consistent with the requirement $(A_{12}^-)^2 = A_{11}^- A_{22}^-$.

It is not immediately obvious why the two (very) different closure approximations should yield the same limiting behaviour for the pair correlation functions as $x_2 \rightarrow 0$. That they do suggests that the limiting behaviour described by Eqs. (18) and (19) should be valid more generally. In the Appendix we show that these results follow from the natural division, Eq. (15), of the pair direct correlation functions into a Yukawa tail plus a short ranged contribution $c_{ij}^{sr}(r)$. Provided the Fourier transforms $\hat{c}_{ij}^{sr}(q)$ are sufficiently well-behaved in the neighbourhood of $q = i\lambda$, Eqs. (18) and (19) should be valid for *any* closure.

V. PHASE DIAGRAM AND LIFSHITZ LINE FOR $\delta = 0.1$

The results presented in the last section imply that within the RPA and HNC introducing a small degree of non-ideality into the pair potentials defining the mixture, i.e. imposing $\delta > 0$, leads to a ‘spinodal’ pole which dictates that pair correlation functions should decay monotonically as $r \rightarrow \infty$ for *all* state points, including those far removed from the spinodal, where one might have expected oscillatory decay (within the HNC). In this section we focus on the spinodal itself and the associated fluid-fluid phase separation.

The spinodal is the locus of points in the phase diagram at which the ‘spinodal’ pole reaches zero. Within the RPA we can determine the spinodal by finding solutions of $\alpha_0^- = 0$, where α_0^- is given by Eq. (10) with the negative sign. This result is plotted in Fig. 4 for $\delta = 0.1$ and $T^* = 1$ (dashed curve). Within the HNC it is not possible to determine the spinodal precisely. For certain densities and concentrations the HNC approximation does not have solutions. However it is possible to calculate the position of the HNC ‘spinodal’ pole as a function of $\rho\lambda^{-3}$ at fixed concentration and extrapolate to zero as shown in Fig. 3. These spinodal points, obtained for a number of concentrations, are shown in Fig. 4 (diamonds). The HNC spinodal lies close to that obtained in the RPA.

Using the RPA we are able to write the reduced bulk Helmholtz free energy per particle, \tilde{f} , as a sum of ideal and excess parts^{4,5,6,7}

$$\tilde{f}(\rho, x_2) = \tilde{f}_{id} + \frac{1}{2}\rho[x_1^2\hat{\phi}_{11}(0) + 2x_1x_2\hat{\phi}_{12}(0) + x_2^2\hat{\phi}_{22}(0)] \quad (20)$$

where $\hat{\phi}_{ij}(0) = 4\pi\epsilon M_{ij}\lambda^{-3}$ is the $q = 0$ limit of the Fourier transformed pair potential. The ideal part, $\tilde{f}_{id}(\rho, x_2)$, contains the ideal free energy of mixing, $\beta^{-1}\{x_1\ln(x_1) + x_2\ln(x_2)\}$, as well as a term in ρ that is irrelevant for phase behaviour. Eq. (20) corresponds to calculating \tilde{f} from the compressibility route, and the spinodal obtained from this equation is identical to that obtained from the zeros of α_0^- . We now Legendre transform to the Gibbs free energy $g = \tilde{f} + Pv$, where $v = 1/\rho$ is the volume per particle and the pressure is given by $P = -(\partial\tilde{f}/\partial v)_{x_2}$. Using the common tangent construction on g we obtain the binodal which is also plotted in Fig. 4 (solid curve). The binodal and spinodal meet at the critical point near $x_2 = 0.27$, $\rho\lambda^{-3} = 0.88$.

In implementing the HNC we choose to calculate the thermodynamic functions locally, thereby avoiding thermodynamic integration. We begin by tracing out isobars across the phase diagram with the pressure given by the virial route:

$$\frac{\beta P}{\rho} = 1 - \frac{2\pi\rho}{3} \sum_i \sum_j x_i x_j \int_0^\infty dr r^3 \frac{d\beta\phi_{ij}(r)}{dr} g_{ij}(r). \quad (21)$$

Along the isobars we calculate the HNC chemical potentials

$$\beta\mu_i = \ln(\rho_i\Lambda_i^3) + \sum_j \rho_j \int d\mathbf{r} \left\{ \frac{h_{ij}(r)}{2} [h_{ij}(r) - c_{ij}(r)] - c_{ij}(r) \right\} \quad (22)$$

where Λ_i is the (irrelevant) thermal de Broglie wavelength of species i , with $i = 1, 2$. The Gibbs free energy per particle is then given by $g = x_1\mu_1 + x_2\mu_2$. By fitting a polynomial to these results we are then able to determine the binodal using the common tangent construction. For the isobars that intersect the region for which the HNC does not provide a solution we calculate the two ‘branches’ of the free energy and construct the common tangent on these; the procedure is equivalent to that used in Ref. 6. Nevertheless, for state points close to the critical point it is not possible to determine the binodal. The HNC binodal is shown in Fig. 4 (crosses connected by tie lines). This lies outside our estimated HNC spinodal and fairly close to the RPA binodal. A slightly better level of agreement between the HNC and RPA results for the binodal was found in Ref. 6 for a softcore model of binary star-polymers.

Since the ‘spinodal’ pole dictates the ultimate decay of the pair correlations even for states that are far removed from the spinodal it is instructive to seek some criterion which indicates when contributions from the other pole(s) become important in determining the structure of the fluid. One valuable indicator of the change in the latter is the Lifshitz line which focuses on the behaviour of the fluid structure at small wave numbers q .^{6,18} We define the partial structure factors as¹⁹

$$S_{ij}(q) = \delta_{ij} + (x_i x_j)^{1/2} \rho \hat{h}_{ij}(q), \quad (23)$$

and concentrate on the number-number structure factor

$$S_{NN}(q) = x_1 S_{11}(q) + x_2 S_{22}(q) + 2(x_1 x_2)^{1/2} S_{12}(q). \quad (24)$$

As we approach the critical point or, indeed, the spinodal, the partial structure factors diverge at small q : $S_{11}(q=0)$ and $S_{22}(q=0) \rightarrow +\infty$ and $S_{12}(q=0) \rightarrow -\infty$. These divergences are reflected in the linear combination, i.e. $S_{NN}(q=0) \rightarrow +\infty$.

We define the Lifshitz line as separating regions of the phase diagram for which $S_{NN}(q)$ has a local maximum or a local minimum at $q=0$. We choose $S_{NN}(q)$ because i) it is the most symmetrical combination of the partial structure factors, and ii) it diverges in a similar manner on both sides of the phase diagram. Formally we make a small q expansion of $S_{NN}(q)$:

$$S_{NN}(q) = a(\rho, x_2) + b(\rho, x_2)q^2 + O(q^4), \quad (25)$$

so that the Lifshitz line is the locus of points for which $b(\rho, x) = 0$.^{6,18} This line is calculated in both the RPA and HNC and the results shown as the dash-dotted curve and crosses, respectively, in Fig. 4. We find that there is good agreement between the two closures, suggesting that in this region of the phase diagram the RPA should become a fairly reliable approximation for describing $h_{ij}(r)$ at both intermediate and large values of r .

VI. DISCUSSION AND CONCLUSIONS

In this paper we have investigated the structural and thermodynamic properties of binary mixtures of particles interacting via purely repulsive (point) Yukawa pair potentials. We have used two approximate closures to the OZ equations in order to calculate the fluid properties: the simple RPA allows us to elucidate analytically some important properties, and the HNC approximation is expected to be very accurate for the Yukawa fluid at the intermediate fluid densities relevant to the present work. This expectation stems from the fact that the HNC closure correlation functions are rather accurate for the OCY.^{9,13}

For the ‘ideal’ mixture, with $\delta = 0$, the RPA approximation gives a poor description of the fluid structure, predicting monotonic (exponential) decay of $rh_{ij}(r)$ for all state points in the phase diagram rather than the Kirkwood crossover line that is manifest in the HNC – see Fig. 2. No fluid–fluid phase separation occurs for $\delta = 0$. By contrast, when $\delta > 0$ an additional purely imaginary pole arises within the HNC approximation for $\hat{h}_{ij}(q)$. This ‘spinodal’ pole governs the phase separation in the mixture for the non–ideal case. Since the RPA provides a good account of this pole – see Fig. 3 – it follows that the RPA also yields fluid–fluid transition boundaries that are quite close to those from the more accurate HNC – see Fig. 4. The amplitude A_{ij}^- of the spinodal pole contribution to $h_{ij}(r)$ becomes increasingly large with increasing proximity to the spinodal, and this

pole provides the dominant contribution in the region of the phase diagram near the spinodal (roughly the region enclosed by the Lifshitz line – see Fig. 4).

For states away from the spinodal/binodal, particularly in the limits $x_1 \rightarrow 0$ or $x_2 \rightarrow 0$, the amplitudes of the contribution from the spinodal pole to the majority species correlation function $h_{ii}(r)$ (where i is the majority species) and to $h_{12}(r)$, become very small – see Figs. 5 and 6. One must magnify the large r tail of these correlation functions in order to see the contribution from the spinodal pole. Above the Kirkwood line, but well away from the spinodal, the intermediate r decay of $h_{ij}(r)$ is damped oscillatory; the oscillations can persist to large r , before the monotonic decay from the spinodal pole finally dominates at very large values of r . This result is quite unusual, since one generally expects the leading order pole to dominate the decay of $h_{ij}(r)$ at both large *and* intermediate values of r .^{9,14,17} In the limit $x_2 \rightarrow 0$, the spinodal pole $\rightarrow i\lambda$ and the amplitudes, A_{11}^- and A_{12}^- , of the contribution of to $h_{11}(r)$ and to $h_{12}(r)$ have a power law dependence on x_2 (see Eq. (19)), vanishing in the pure fluid of species 1. However, the amplitude, A_{22}^- , of the contribution from the spinodal pole to $h_{22}(r)$ tends to a non–vanishing value in the limit $x_2 \rightarrow 0$. This means that for small values of x_2 the nature of the decay of the correlation function $h_{22}(r)$ can be very different from that of $h_{11}(r)$ and $h_{12}(r)$, a situation which has not been encountered in other fluid mixtures. In experimental or simulation results it would be almost impossible to detect the contribution in $h_{11}(r)$ and $h_{12}(r)$ from the ‘spinodal’ pole for small x_2 . However, its existence could be inferred from the apparently different decay of $h_{22}(r)$ versus that of $h_{11}(r)$ and $h_{12}(r)$.

It is important to emphasise that the amplitude A_{22}^- tending to a non-zero value in the limit $x_2 \rightarrow 0$ does not imply any pathological consequences for thermodynamic or measurable structural quantities. As pointed out earlier, physical observables such as the liquid structure factors involve the product $\rho_2 h_{22}(r)$ which vanishes as $x_2 \rightarrow 0$. One exception to this rule is the effective potential between two particles immersed in a solvent of the other species. The effective potential $\phi_{22}^{eff}(r)$ between two particles of species 2 at infinite dilution is related to the radial distribution function, in the limit $x_2 \rightarrow 0$, by

$$g_{22}(r) \equiv \exp(-\beta\phi_{22}^{eff}(r)). \quad (26)$$

Clearly $\phi_{22}^{eff}(r)$ depends on the density and temperature of the solvent (species 1). We define the solvent-mediated potential $W_{22}(r)$ via $\phi_{22}^{eff}(r) \equiv \phi_{22}(r) + W_{22}(r)$, where $\phi_{22}(r)$ is the bare (direct) potential between the two particles. $W_{22}(r)$ depends on the nature of the solvent and on the solvent-particle interaction. From Eq. (26) it follows that $W_{22}(r)$ depends on $h_{22}(r)$ rather than $\rho_2 h_{22}(r)$. There are clear implications for the form of $\phi_{22}^{eff}(r)$ given that the amplitude of the contribution to $h_{22}(r)$ from the spinodal pole is non–vanishing in the limit $x_2 \rightarrow 0$. We leave a full discussion to another publication but point

out that the presence of the spinodal pole, which occurs for any $\delta > 0$, gives rise to an effective potential that is *attractive* at sufficiently large distances and decays as $\exp(-\lambda r)/r$, i.e. with the same length scale as the bare potentials.

Given that the Yukawa potential arises in a great variety of physical problems,²⁰ typically where there are big charged particles screened by a neutralising background medium, we believe the present work should be relevant to systems ranging from charged colloidal fluids¹ to dusty plasmas.²

We have chosen to focus on a simple example of a binary Yukawa mixture, namely one in which the inverse screening length λ is the same for all ij pairs, as this is the situation which arises naturally for charged particles immersed in a neutralising medium. One could, of course, consider more complex examples with λ dependent on the species indices i, j . Moreover, one could consider mixtures that correspond to *negative* non-additivity, i.e. with $\delta < 0$. In this case $M_{12} < \sqrt{M_{11}M_{22}}$ and the interactions should favour fluid-fluid mixing.

Acknowledgements

PH is grateful for the support of an EPSRC studentship and AJA acknowledges the support of EPSRC under grant number GR/S28631/01.

Appendix: Behaviour of correlation functions as $x_2 \rightarrow 0$

Here we show that the results for the spinodal pole and the amplitudes A_{ij}^- , Eqs. (18) and (19), in the limit $x_2 \rightarrow 0$ are not specific to the RPA but follow generally from the form of the direct correlation functions for Yukawa mixtures. Making the separation of the $c_{ij}(r)$ given by Eq. (15) and substituting into Eq. (5) we obtain

$$D(q) = a + \frac{b}{p} + \frac{c}{p^2}, \quad (27)$$

where

$$\begin{aligned} p &= q^2 + \lambda^2, \\ a &= [1 - \rho_1 c_{11}^{sr}(q)][1 - \rho_2 c_{22}^{sr}(q)] - \rho_1 \rho_2 [c_{12}^{sr}(q)]^2 \\ b &= [1 - \rho_1 c_{11}^{sr}(q)]\rho_2 \alpha_{22} + [1 - \rho_2 c_{22}^{sr}(q)]\rho_1 \alpha_{11} \\ &\quad + 2\rho_1 \rho_2 c_{12}^{sr}(q)\alpha_{12}, \\ c &= \rho_1 \rho_2 (\alpha_{11}\alpha_{22} - \alpha_{12}^2) \end{aligned} \quad (28)$$

and $\alpha_{ij} = 4\pi M_{ij}/\lambda T^*$. The poles are given by the solution to the equation $D(q) = 0$. From equation (27), we see that one set of solutions is given by

$$p_{\pm} = -(b \pm \sqrt{b^2 - 4ac})/2a. \quad (29)$$

a and b are functions of q . However, Eq. (29) leads to purely imaginary poles at $q_{\pm} = i\alpha_0 = i\sqrt{\lambda^2 - p_{\pm}}$, provided we assume that the functions $c_{ij}^{sr}(q)$ are well behaved (finite and differentiable) on the imaginary axis around q_{\pm} . The leading order pole is that corresponding to p_- , which in the limit of vanishing density $\rho_2 = 0$ (i.e. $c = 0$) yields a pole at $q = i\lambda$, giving a decay $rh_{ij}(r) \sim A_{ij}^- \exp(-\lambda r)$, where the amplitudes A_{ij}^- are to be determined below. For small concentrations of species 2 we can Taylor expand p_- in powers of c , giving

$$p_- = -\frac{c}{\rho_1 \alpha_{11}} + \left(\frac{c(b - \rho_1 \alpha_{11})}{\rho_1^2 \alpha_{11}^2} - \frac{ac^2}{\rho_1^3 \alpha_{11}^3} \right) + O(\rho_2^3). \quad (30)$$

We find that in the limit $\rho_2 \rightarrow 0$, $p_- \sim -(\alpha_{22} - \alpha_{12}^2/\alpha_{11})\rho_2$. Thus the leading order pole has

$$\alpha_0^- = \lambda \left(1 - \frac{\alpha_{11}\alpha_{22} - \alpha_{12}^2}{2\lambda^2 \alpha_{11}} \rho_2 \right) + O(\rho_2^2), \quad (31)$$

which is identical to the RPA result in Eq. (18).

The amplitude, A_{ij}^- is given by:

$$A_{ij}^- = \frac{q_- N_{ij}(q_-)}{2\pi D'(q_-)}, \quad (32)$$

where the prime denotes the derivative with respect to q and the functions $N_{ij}(q)$ are given in Eq. (6). From Eq. (27) we find that

$$D'(q) = a' + \frac{b'}{p} - \frac{2qb}{p^2} - \frac{4qc}{p^3}. \quad (33)$$

In the limit $\rho_2 \rightarrow 0$, using (30), we find that $D'(q_-) = 2q_- b/p_-^2$ + other terms less singular in ρ_2 . Using this result, we can expand in Eq. (32) to obtain the amplitudes A_{ij}^- in the limit $\rho_2 \rightarrow 0$. We find that the leading order terms are precisely the RPA results given in Eq. (19) – i.e. in the limit $\rho_2 \rightarrow 0$ the amplitudes A_{ij}^- are independent of the functions $\hat{c}_{ij}^{sr}(q)$.

* Paul.Hopkins@bristol.ac.uk

† Andrew.Archer@bristol.ac.uk

¹ See, e.g. J.-P. Hansen and H. Löwen, *Annu. Rev. Phys. Chem.* **51**, 209 (2000) and references therein

² For a recent review see A. Piel and A. Melzer, *Adv. Space Res.*, **29**, 1255 (2002), and references therein

³ J.-P. Hansen and I.R. McDonald, *Theory of Simple Liquids*, Academic, London, (1986), 2nd ed.

- ⁴ A.A. Louis, P.G. Bolhuis and J.-P. Hansen, Phys. Rev. E. **62**, 7961 (2000)
- ⁵ A.J. Archer and R. Evans, Phys. Rev. E. **64**, 041501 (2001)
- ⁶ A.J. Archer, C.N. Likos, and R. Evans, J. Phys.: Cond. Mat. **14**, 12031 (2002)
- ⁷ R. Finken, J.-P. Hansen and A.A. Louis, J. Stat. Phys. **110**, 1015 (2003)
- ⁸ M. Baus and J.-P. Hansen, Phys. Rep. **59**, 1 (1980) and references therein.
- ⁹ P. Hopkins, A.J. Archer and R. Evans, Phys. Rev. E **71** 027401 (2005)
- ¹⁰ C.N. Likos, Phys. Rep. **348**, 267 (2001)
- ¹¹ C.N. Likos, A. Lang, M. Watzlawek and H. Löwen, Phys. Rev. E **63**, 031206 (2001)
- ¹² A. Lang, C.N. Likos, M. Watzlawek and H. Löwen, J. Phys.: Condens. Matter **12**, 5087 (2000)
- ¹³ W. Daughton, M.S. Murillo and L. Thode, Phys. Rev. E **61**, 2129 (2000)
- ¹⁴ R. Evans, R.J.F. Leote de Carvalho, J.R. Henderson and D.C. Hoyle, J. Chem. Phys. **100**, 591 (1994); see also G. A. Martynov, *Fundamental Theory of Liquids: Methods of Distribution Functions* (Hilger, Bristol, 1992)
- ¹⁵ Note that the RPA results of Eqs. (11) and (13) predict unphysical behaviour of $h_{ij}(r)$ as $r \rightarrow 0$. However, we are concerned here with $h_{ij}(r)$ as $r \rightarrow \infty$ where the RPA results do capture the essential physics.
- ¹⁶ J.G. Kirkwood, Chem. Rev. (Washington, D.C.) **19**, 275 (1936)
- ¹⁷ R.J.F. Leote de Carvalho, R. Evans and Y. Rosenfeld, Phys. Rev. E **59**, 1435 (1999)
- ¹⁸ G. Gompper and M. Schick, Phys. Rev. B **41**, 9148 (1990); R.M. Hornreich, R. Liebmann, H.G. Schuster and W. Selke, Z. Phys. B **35**, 91 (1979)
- ¹⁹ See, e.g. C. Caccamo, Phys. Rep. **274**, 1 (1996) and references therein
- ²⁰ J.S. Rowlinson, Physica A, **156**, 15 (1989)